

SYNERGISTIC EXTRACTION AND TRANSPORT OF Pb(II) AND Cu(II) THROUGH POLYMERIC MEMBRANES USING A MIXTURE OF D2EHPA AND TOPO IN THE PRESENCE OF EDTA

SIHAM CHELOUAOU and FATMA SADI

Laboratory of Electrochemistry-Corrosion, Metallurgy and Mineral Chemistry, Faculty of Chemistry, University of Sciences and Technology Houari Boumediene (USTHB), PO Box 32, El Alia Bab -Ezzouar 16111, Algiers, Algeria

✉ *Corresponding author: S. Chelouaou, sihamchelouaou@yahoo.fr*

Received November 10, 2024

In this work, we studied the synergistic extraction and transport of Copper (II) and Lead (II) through polymeric membranes using two polymers, such as methyl methacrylate (PMMA) and cellulose triacetate (CTA), as polymeric matrix. A mixture of two extractants, di-(2-ethylhexyl) phosphoric acid (D2EHPA) and tri-octylphosphine oxide (TOPO), in a 1:1 volume ratio, was used as a specific carrier. This extractant mixture forms stable metal complexes, thereby enhancing the selective transport of the target ions. Coupling the process with EDTA in the strip phase further improves the recovery of Pb^{2+} and Cu^{2+} , while minimizing back-diffusion, plasticized with di-octyl phthalate (DOP) by the solvent evaporation method. The membranes were characterized using Fourier transform infrared spectroscopy (FTIR), contact angle measurement, scanning electron microscopy (SEM) and thermogravimetric analysis (TGA-DSC). This new approach combines the specific characteristics of extractants (D2EHPA/TOPO) with the advantages of plasticized polymer membranes, which enable heavy metals to be separated and concentrated. An effective and environmentally sustainable solution is proposed thanks to the properties of the extractants and the characteristics of the plasticized polymer membranes. This method offers an effective, sustainable and ecological solution for more responsible management of metal resources and environmental protection.

Keywords: polymeric membranes, synergetic extraction, D2EHPA/TOPO, transport, CTA/PMMA

INTRODUCTION

The presence of trace heavy metals in wastewater is a serious environmental issue. These compounds, which come mainly from industrial waste, agricultural practices and the domestic use of chemicals, pose significant challenges in terms of treating and protecting water resources.¹ For example, lead and copper are found in products such as paints, water pipes and certain cosmetics. This is especially true in developing countries. Due to its conductive properties, copper is used in many electrical and electronic products.² In this context, it is becoming imperative to explore innovative and sustainable solutions in order to strengthen environmental regulations and develop treatment infrastructures.

In recent decades, environmental regulations have become stricter regarding industrial activities involving heavy metals. Also, focusing on the treatment of wastewater, recently, significant

attention has been given to purification-concentration techniques, such as membrane separation³⁻⁵ and synergistic extraction.⁶⁻⁸ Various methods for the extraction of metal ions from aqueous solutions have been developed, including solvent extraction,⁸ chemical precipitation,⁹ coagulation,¹⁰ ion exchange,¹¹ adsorption,¹³ and membrane-based methods, such as ultrafiltration,⁵ electrodialysis,¹⁴ bulk liquid membranes (BLM),¹⁵ supported liquid membranes (SLM),¹⁶⁻²² emulsion liquid membranes (ELM),¹⁷ and polymer inclusion membranes (PIM).¹⁸⁻²⁶ A wide range of compounds, from anions or metal species to small organic molecules, have been extracted using PIMs.²⁰⁻²⁶

The present study introduces innovative membranes developed by poly(methyl methacrylate) (PMMA) and cellulose triacetate (CTA), incorporating dioctyl phthalate (DOP) as a

plasticizer. These membranes include a neutral extracting agent (TOPO) and a cationic extracting agent (di(2-ethylhexyl) phosphate, D2EHPA) as liquid carriers. The research focuses on investigating the transport of metallic cations, specifically Cu^{2+} and Pb^{2+} , through these polymeric membranes.

Affinity membranes are gaining attention due to their ease of preparation, cost-effectiveness, versatility, improved stability, and high efficiency. The study aims to enhance the transport efficiency of heavy metals to the strip compartment by leveraging the advantages of D2EHPA/TOPO extractants and polymeric membranes. This involves optimizing parameters, such as pH, transport duration, and the composition of the receiving solution, to achieve selective transport of Cu^{2+} and Pb^{2+} .

In the field of membrane-based separation, the choice of extractants is critical to ensure high selectivity and efficiency. The combination of D2EHPA (bis(2-ethylhexyl) phosphoric acid) and TOPO (tri-n-octylphosphine oxide) is well documented for its synergistic behavior in the extraction of metal ions, especially uranium and iron, and is industrially exploited in the URPPOS process. This synergistic effect arises from the formation of highly stable metal-extractant complexes. In this work, the D2EHPA/TOPO system is coupled with EDTA in the strip compartment to enhance metal recovery and prevent back-diffusion, offering a promising approach for the selective transport of Pb^{2+} and Cu^{2+} through polymer inclusion membranes.

The characterization of the developed membranes was performed by various analytical techniques, including contact angle measurement, Fourier-transform infrared spectroscopy (FTIR), scanning electron microscopy (SEM), and thermogravimetric analysis (TGA-DSC). These

methods provide insights into membrane structure, surface properties, and thermal behavior, crucial for assessing their suitability in metal ion transport applications.

EXPERIMENTAL

Reagents and solutions

Polymethyl methacrylate (PMMA) pellets and cellulose triacetate (CTA) pellets were obtained from Acros (USA). Di-(2-ethylhexyl) phosphoric acid (D2EHPA) (99%), tri-n-octylphosphine oxide (TOPO) (98%), and lead(II) nitrate ($\text{Pb}(\text{NO}_3)_2$) (99%) were sourced from Fluka (Germany). Copper(II) chloride (CuCl_2) (99.99%) was obtained from Merck (Germany), and chloroform (99%) was received from VWR Chemicals. Dioctyl phthalate (DOP) (99.5%) was a product of Carlo Erba (Val de Reuil, France). Hydrochloric acid (HCl) (37%, $d = 1.18$, Carlo Erba), ethylenediamine tetraacetic acid (EDTA) (98% Fluka) and sodium chloride (NaCl) (100.4%, Carlo Erba) were used. Sodium hydroxide (NaOH) (98%, Carlo Erba) was also used.

Deionized water was used to prepare all aqueous solutions. Aqueous solutions of Pb and Cu were prepared by dissolution in an HCl solution. Highly purified water was used for the preparation of the aqueous solutions, and the real sample was diluted to provide a suitable test solution.

Preparation method of membranes

The polymeric membranes were prepared by the method described by Sugiura.^{30,31} To prepare the membranes, we dissolved a precise quantity of 0.1 g of each polymer: polymethyl methacrylate (PMMA) and cellulose triacetate (CTA), in 15 mL of chloroform, under stirring for several hours, to obtain a homogeneous polymer solution. After 2 hours, we added the necessary quantities of the components and 0.1 mL of DOP. The D2EHPA/TOPO mixture was prepared using a volumetric ratio of 1:1, meaning that equal volumes of D2EHPA and TOPO were mixed together into this polymer solution, stirring constantly to ensure uniform dispersion of the extractants and plasticizer.

Table 1
Composition of membranes

Membranes composition.	PMMA (g)	CTA (g)	DOP (mL)	D2EHPA/TOPO
PMMA+DOP	0.2	/	0.1	/
CTA+DOP	/	0.2	0.1	/
PMMA+CTA+DOP	0.1	0.1	0.1	/
PMMA+ DOP+ D2EHPA+TOPO	0.2	/	0.1	0.1
CTA+DOP+ D2EHPA+TOPO	/	0.2	0.1	0.1
PMMA+ CTA+DOP+D2EHPA+TOPO	0.1	0.1	0.1	0.1

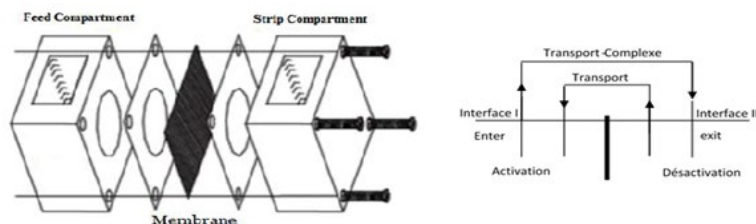


Figure 1: Transport cell scheme

The resulting solution was then poured into a clean glass Petri dish to form a uniform film. The solvent was allowed to evaporate at room temperature for 24 hours to obtain solid membranes. Finally, the dry membranes were gently peeled off the glass plate to be used in the extraction and transport experiments. Table 1 presents the membrane compositions.

Experimental process for transporting lead (II) and copper (II) through polymeric membranes

The transport of lead (II) and copper (II) through modified polymer membranes was carried out in a Plexiglas cell shown in Figure 1. In the feed compartment, a solution containing the metal ions to be extracted (Cu^{2+} and Pb^{2+}) in an acidic medium is introduced, while the strip compartment contains an EDTA ($5 \cdot 10^{-3} \text{M}$) solution adjusted to a pH of around 10 to facilitate the complexation and transport of the metals. The two compartments are brought into contact via a polymeric membrane impregnated with a mixture of extractants.

Speciation diagram of lead (II) and copper (II)

The extracted species were determined using the species distribution diagrams drawn by the computer program Medusa, chemical equilibrium diagram software (version: Eq. calcs_32).

Medusa software (in combination with Hydra) was used to simulate chemical equilibria. The chemical species were selected based on equilibrium constants

from the software's built-in database. Simulation conditions (pH, concentration, temperature) were defined to match the experimental setup.

Figure 2 shows the distribution pattern of the chlorinated Pb (II) complexes at the concentration of Lead (II) 0.48 mM (0.1 g/L) and the concentration of chloride ions of 500 mM at 25 °C. Chlorinated lead (II) complexes have been distributed at pH below 6 and the extractants can react with these ionic substances (Pb^{2+} , PbCl_2 , PbCl_3^- and PbCl_4^{2-}) to form complexes. The formation reactions and their equilibrium constants are the following:

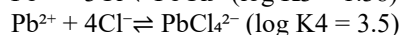
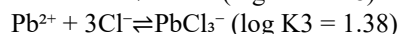


Figure 3 shows the distribution pattern of chlorinated copper (II) complexes at a copper (II) concentration of 0.74 mM (0.1 g/L) and a chloride ion concentration of 500 mM, we need to consider the speciation of copper in the presence of chloride ions. Copper (II) can form various complexes with chloride ions, such as CuCl^+ , CuCl_2 , CuCl_3^- , and CuCl_4^{2-} , depending on the concentrations and the stability constants of these complexes. The formation reactions and their equilibrium constants are shown below:

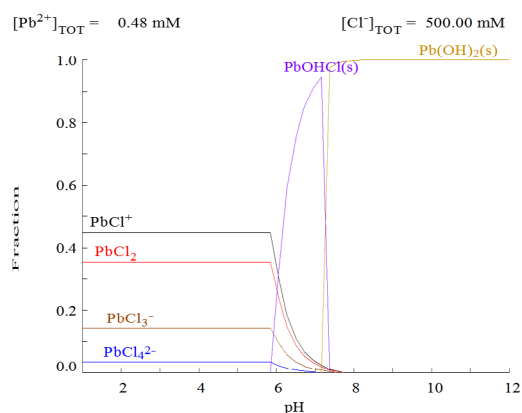
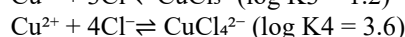
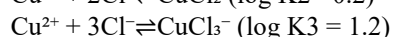
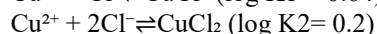
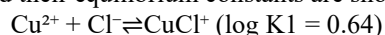


Figure 2: Distribution pattern of chlorinated Pb (II) complexes

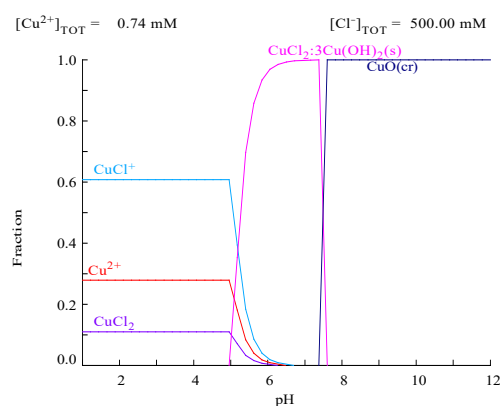


Figure 3: Distribution pattern of chlorinated copper (II) complexes

RESULTS AND DISCUSSION

Contact angle measurements

The determination of contact angles of the various elaborated membranes provides valuable insights into the surface state and surface tensions of the materials. This characterization helps to ascertain the hydrophobic/hydrophilic nature of the different polymeric membranes. Table 2 summarizes the values of contact angles and densities of the various elaborated cellulose membranes.

The PMMA+DOP+D2EHPA+TOPO blend has a contact angle of 62.7° , indicating that the surface is hydrophilic. This means that the surface has a high affinity for water, which spreads easily over it. In contrast, the CTA+DOP+D2EHPA+TOPO mixture has a contact angle of 117° , indicating that the surface is hydrophobic. In general, a surface is considered hydrophobic if the contact angle is greater than 90° , which means that water does not spread easily over it. Finally, the PMMA+CTA+DOP+D2EHPA+TOPO blend has a contact angle of 78° , also indicating that the surface is hydrophilic, although the affinity for water is less marked than in the case of the first blend.

Characterization of synthesized membranes by Fourier transform infrared spectroscopy (FTIR)

Fourier Transform Infrared Spectroscopy (FTIR) allows the identification of different functional groups present in each compound. Its high sensitivity makes it possible to study the molecular behavior and movements of polymer chains at a microscopic level. This advanced technique also facilitates the identification and quantification of the various interactions that can occur between the different constituents of a membrane (polymer, plasticizer and extractant).

We have observed that the FTIR spectra of the membranes, grouped in Figures 4, 5, and 6 show distinct bands that can be attributed to specific functional groups of the cellulose triacetate (CTA) and PMMA polymers, the D2EHPA and TOPO carriers, the DOP plasticizer, and the complexing agent.

The presence of bands at 2957 cm^{-1} , 2930 cm^{-1} , and 2865 cm^{-1} is attributed to, respectively, the asymmetric and symmetric vibrations of the C-H and $\text{-CH}_2\text{-}$ bonds. The peaks at 1270 cm^{-1} and 1069 cm^{-1} are attributed to the asymmetric and symmetric vibrations of the C-O-C group, respectively.

Table 2
Contact angle and density of the membranes produced

Membrane	Contact angle ($^\circ$)	Density (mg/cm^2)
PMMA+DOP+D2EHPA+TOPO	62.88	1.18
CTA+DOP+D2EHPA+TOPO	117	1.22
PMMA+CTA+DOP+D2EHPA+TOPO	78	1.2

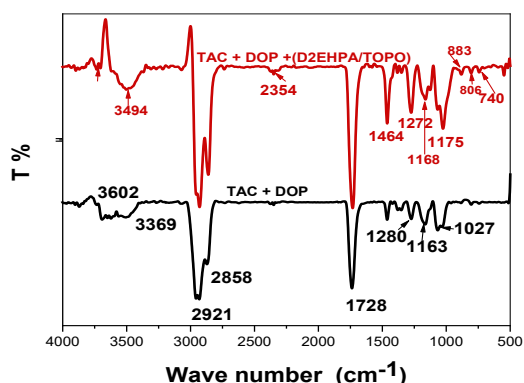


Figure 4: FTIR spectra of membranes CTA+DOP and CTA+DOP+D2EHPA/TOPO

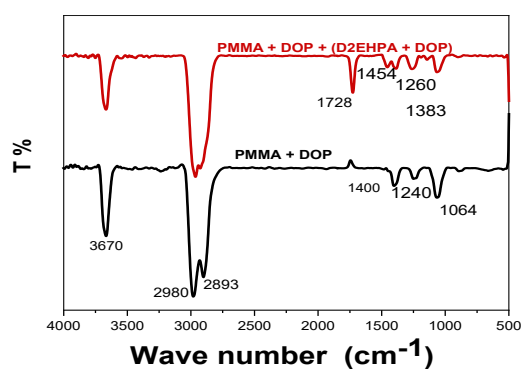


Figure 5: FTIR spectra of membranes PMMA+DOP and PMMA+DOP+D2EHPA/TOPO

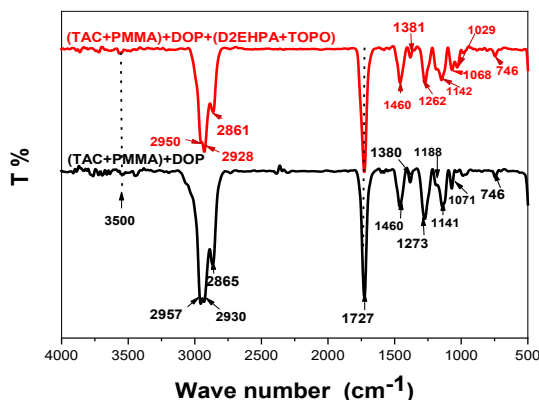
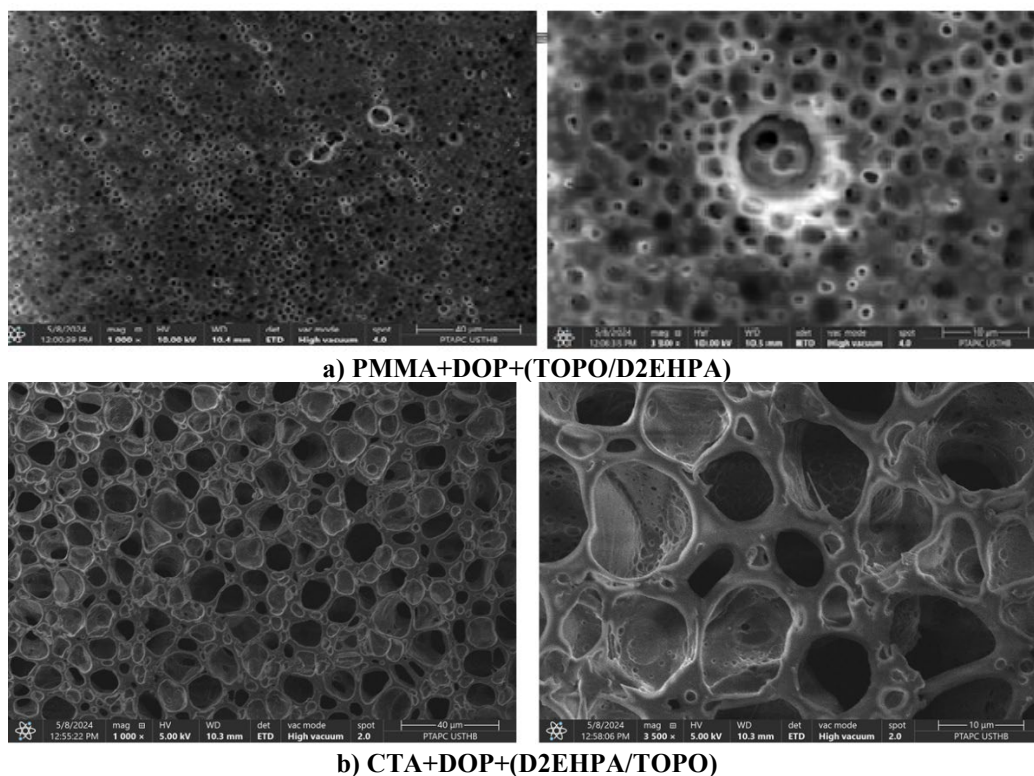


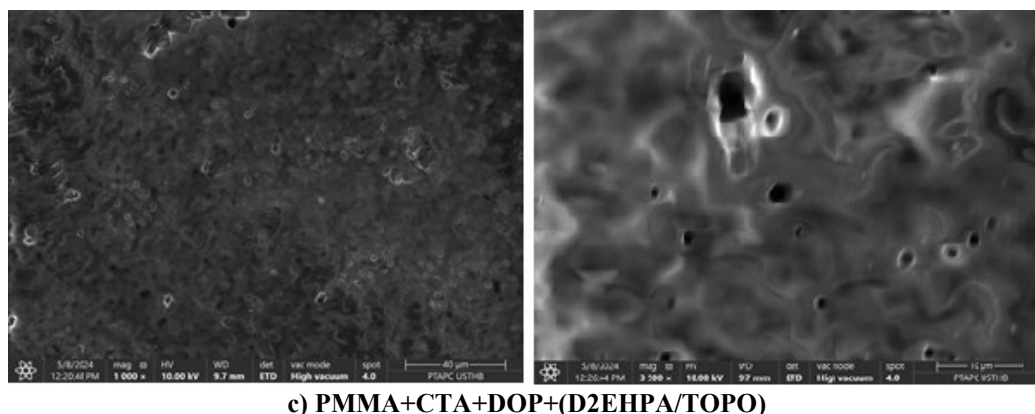
Figure 6: FTIR spectra of membranes CTA+PMMA+DOP and CTA+PMMA+DOP+D2EHFA/TOPO

The main absorption band is detected at 1728 cm^{-1} , corresponding to the carbonyl $\text{C}=\text{O}$ group vibration in the DOP and CTA/PMMA polymers. Additionally, two bands at 1460 cm^{-1} and 746 cm^{-1} were also observed, corresponding to the angular deformation of the $-\text{CH}_2$ and $-\text{CH}$ groups of the DOP plasticizer. Finally, a band at 1142 cm^{-1} corresponds to the characteristic stretching vibration of the $\text{C}-\text{O}-\text{C}$ group in PMMA.

Characterization by scanning electron microscopy (SEM)

A scanning electron microscope (SEM) was used to determine the morphology of the membranes. Membrane samples were prepared by freezing under liquid nitrogen (70 K) and rapidly fracturing them, resulting in a clean fracture to visualize their cross-section. The samples were mounted with conductive adhesive on metal supports, with the fractured side facing upwards, and then sputter-coated with gold. The samples were then observed using SEM at magnifications ranging from around $1000\times$ to $3500\times$.





c) PMMA+CTA+DOP+(D2EHPA/TOPO)

Figure 7: Scanning electron microscopy images of the synthesized membranes

The scanning electron microscopy (SEM) observations show that all the membranes produced have a non-homogeneous pore structure. This is probably due to the addition of the plasticizer DOP and the presence of the extractants D2EHPA and TOPO in the composition of the membranes, which can affect the formation of pores and porous cavities in the polymer matrix. By adding plasticizers, such as DOP, and extractants, such as D2EHPA and TOPO, the polymer matrix is disrupted, leading to pore formation. This disruption manifests itself in the form of cavities and spaces within the polymer matrix.

Thermogravimetric (TGA) and dTG analyses

Thermogravimetric analysis (TGA) was applied to evaluate the thermal stability of the membrane components. TGA is a reliable technique for monitoring thermal decomposition processes, including evaporation, desorption, sublimation, oxidation, and reduction. The measurements were conducted using a TA Instruments TGA Q500 system, programmed from

50 to 500 °C, at a constant heating rate of 10 °C/min under nitrogen atmosphere.

A detailed thermal analysis was carried out on a membrane composed of cellulose triacetate (CTA), polymethyl methacrylate (PMMA), and plasticized with dioctylphthalate (DOP). This membrane was modified by the addition of specific transporters, di-2-ethylhexylphosphoric acid (D2EHPA) and trioctylphosphine oxide (TOPO). The thermal and decomposition properties of the membrane were studied using differential thermogravimetric analysis (dTG) and thermogravimetric analysis (TGA). The results obtained are shown in Figures 8-10.

The TGA curve shows losses of sample weight as a function of temperature. An initial decrease in weight at lower temperatures (up to around 100 °C) may indicate the loss of volatile components or moisture. Significant weight loss occurs between 200 °C and 400 °C, which may be associated with thermal decomposition of membrane components. Typically, cellulose triacetate begins to decompose around 300-350 °C, DOP volatilizes at around 230-300 °C.³⁰

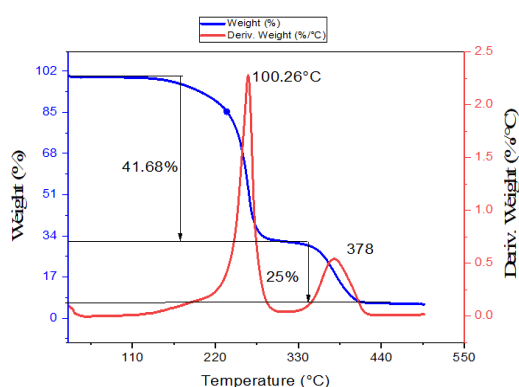


Figure 8: Thermogravimetric (TGA) and (dTG) curves of elaborated membranes PMMA + DOP + (D2EHPA/TOPO)

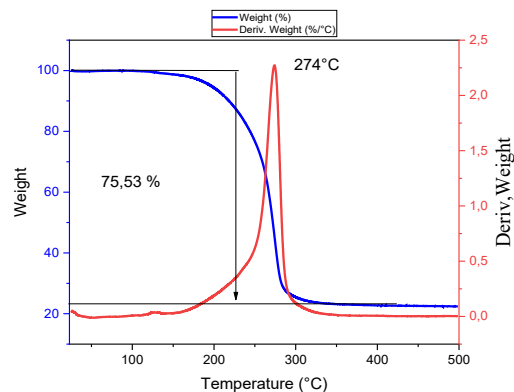


Figure 9: Thermogravimetric (TGA) and dTG curves of membranes CTA + DOP + (D2EHPA/TOPO)

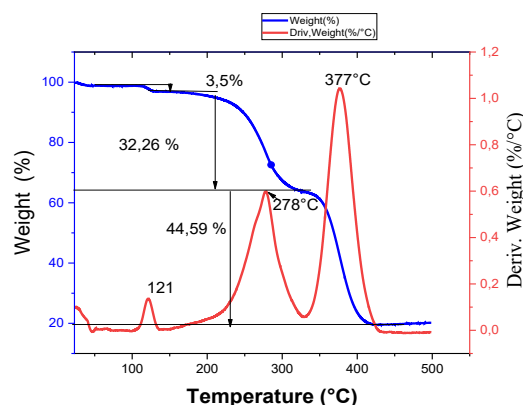


Figure 10: Thermogravimetric (TGA) and dTG curves of membranes CTA+PMMA + DOP + (D2EHFA/TOPO)

The dTG curve shows the rate of weight change. The peaks in this curve represent the temperatures where mass loss is most rapid. The main peaks at around 250 °C and 350 °C may indicate the main decompositions of DOP and cellulose triacetate (CTA), respectively.³⁰

In Figure 10, the mass loss evolution as a function of temperature for the membrane composed of cellulose triacetate (CTA) and PMMA polymers, with the plasticizer DOP is illustrated. The degradation process clearly follows three steps. An initial mass loss of approximately 3.5% occurs between 100-150 °C, attributed to the evaporation of the plasticizer (DOP). A second, more significant mass loss of around 32.26%, is observed, with a peak degradation temperature near 278 °C, spanning the temperature range from 250 °C to 300 °C. This stage is associated with the degradation of the cellulose triacetate (CTA) polymer. The final degradation stage, representing a mass loss of about 44.59%, begins around 400 °C. This stage corresponds to the breakdown of PMMA and D2EHFA. A residual weight loss beyond 400 °C could indicate the decomposition of more stable components such as TOPO.

Transport study of two metal cations, Pb^{2+} and Cu^{2+} , across plasticized polymeric membranes

Using the transport cell described in Figure 1, we studied the active transport of $\text{Pb}(\text{II})$ and $\text{Cu}(\text{II})$ across the plasticized polymer membranes. The assay was carried out by atomic absorption on samples taken from the feed compartment and the strip compartment over a 24-hour period.

Investigation of Pb^{2+} and Cu^{2+} in the feed compartment over time

To study the effect of the presence of a complexing agent in the strip compartment on the

transport of $\text{Pb}(\text{II})$ and $\text{Cu}(\text{II})$ ions, we maintained the metal concentration in the feed phase at 100 mg/L in a hydrochloric acid medium (0.5 M). The receiving phase contained an EDTA solution (510^{-3}M), which serves to trap metal ions in the form of stable complexes, ensuring efficient, irreversible, and selective transport of metals across the membrane.

Figures 11 and 12 show the variation in $\text{Pb}(\text{II})$ and $\text{Cu}(\text{II})$ ions concentrations in the feed compartment over time, using three membranes that differ in the nature of the base polymers: CTA+PMMA+DOP+(D2EHFA/TOPO), CTA+DOP+(D2EHFA/TOPO), and PMMA+DOP+(D2EHFA/TOPO). The results show that the membranes used have different capacities for the transport of these metals.

The results of the study show significant variations in the efficiency of the membranes for transporting $\text{Pb}(\text{II})$ ions depending on the nature of the base polymers used. For the CTA+PMMA+DOP+(D2EHFA/TOPO) membrane, the $[\text{Pb}^{2+}]$ concentration decreases rapidly at the start, stabilizing at around 40 mg/L after about 6 hours, indicating a high initial efficiency that reaches a plateau relatively quickly. In contrast, the CTA+DOP+(D2EHFA/TOPO) membrane shows a strong continuous decrease in $[\text{Pb}^{2+}]$ concentration, reaching around 0 mg/L after 24 hours, demonstrating exceptional efficiency in removing $[\text{Pb}^{2+}]$ from solution. Finally, the PMMA+DOP+(D2EHFA/TOPO) membrane shows a rapid decrease in $[\text{Pb}^{2+}]$ concentration initially, followed by a slower decrease, reaching approximately 40 mg/L after 24 hours, reflecting moderate efficiency.

The curve in Figure 12 shows the concentration of $[\text{Cu}^{2+}]$ (mg/L) as a function of time (h) for the three different membranes. Membrane

CTA+PMMA+DOP+(D2EHPA/TOPO) shows a gradual reduction in Cu(II) concentration from 100 mg/L to approximately 28 mg/L after 24 hours. CTA+DOP+(D2EHPA/TOPO) demonstrates a rapid and efficient reduction, decreasing from 100 mg/L to 0 mg/L within 5 hours and maintaining at 0 mg/L. PMMA+DOP+(D2EHPA/TOPO) shows

initial fluctuations before gradually decreasing from 100 mg/L to about 15 mg/L after 24 hours. These observations confirm that the CTA+DOP+(D2EHPA/TOPO) membrane is the most effective in reducing Cu(II) concentrations, while the other membranes show varying efficiencies.

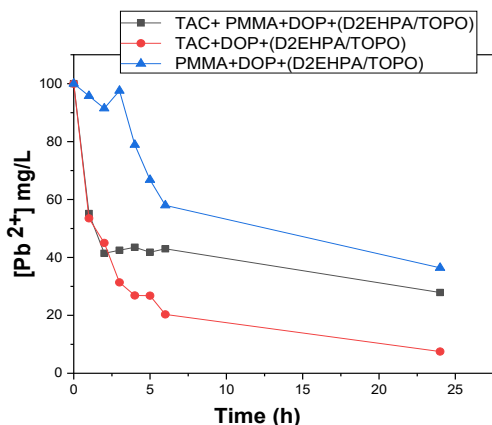


Figure 11: Variations in Pb^{2+} concentration as a function of time in the feed compartment ($[Pb^{2+}]_I = 100$ mg/L, $[EDTA]_{II} = 5.10^{-3}$ M)

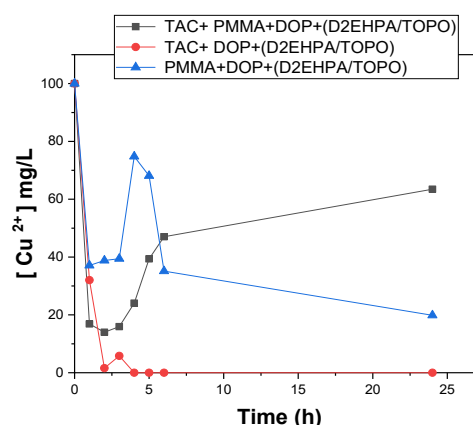


Figure 12: Variations in Cu^{2+} concentration as a function of time in the feed compartment ($[Cu^{2+}]_I = 100$ mg/L, $[EDTA]_{II} = 5.10^{-3}$ M)

Investigation of Pb(II) and Cu(II) concentration in the strip compartment over time

The system containing CTA+PMMA+DOP+(D2EHPA/TOPO) appears to be the most effective at retaining or complexing Pb^{2+} , with the concentration increasing significantly over time. On the other hand, the system with CTA+DOP+(D2EHPA/TOPO) is the

least efficient, showing a concentration of Pb^{2+} stable at zero, which could indicate an absence of adsorption or a very low efficiency of this system. Finally, the system with PMMA+DOP+(D2EHPA/TOPO) shows an intermediate performance, with an initial increase followed by a stabilization of the Pb^{2+} concentration.

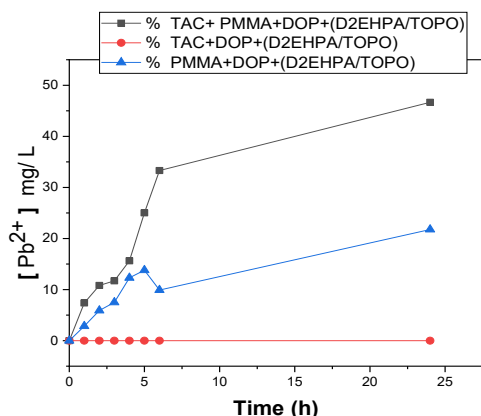


Figure 13: Variation of Pb (II) concentration in the strip compartment vs time across the synthesized membranes ($[Pb^{2+}]_I = 100$ mg/L, $[EDTA]_{II} = 5.10^{-3}$ M)

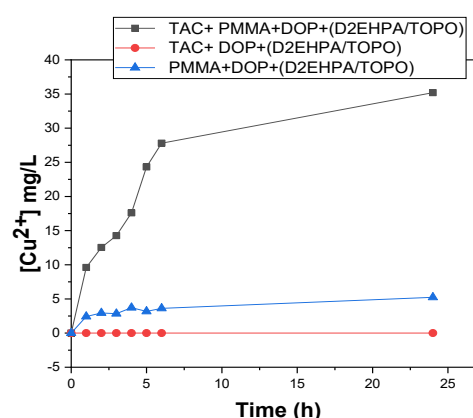


Figure 14: Variation of Cu(II) concentration in the strip compartment vs time across the synthesized membranes ($[Cu^{2+}]_I = 100$ mg/L, $[EDTA]_{II} = 5.10^{-3}$ M)

The results for Cu(II) ion transport show distinct behavior depending on the membranes used. The CTA+PMMA+DOP+(D2EHPA/TOPO) membrane shows a rapid increase in Cu^{2+}

concentration, reaching around 35 mg/L after 24 hours, indicating that this combination strongly favors the increase in Cu^{2+} . In contrast, the CTA+DOP+(D2EHPA/TOPO) membrane

maintains an almost flat curve around 5 mg/L throughout the experiment, meaning that this combination has no significant effect on Cu^{2+} concentration.

The PMMA+DOP+(D2EHPA/TOPO) membrane shows a slight increase in Cu^{2+} concentration, reaching around 10 mg/L after 24 hours, indicating a moderate effect on the increase in Cu^{2+} , but less pronounced than that observed with the first combination.

Once saturated with metal ions, the membrane can theoretically be regenerated through a desorption process, typically involving treatment with an acidic solution, such as HCl or HNO_3 . This procedure facilitates the release of the adsorbed metal ions, thereby contributing to the extension of the membrane's operational lifespan. Alternatively, an electrolysis process may also be considered for effective regeneration.

CONCLUSION

In the initial phase of this study, separation membranes were developed using cellulose triacetate (CTA) and polymethyl methacrylate (PMMA) as the polymeric matrix, dioctyl phthalate (DOP) as the plasticizer, and D2EHPA/TOPO as the carrier. The membranes were characterized using SEM, Fourier-transform infrared spectroscopy (FTIR), contact angle and thermogravimetric analysis (TGA-DTG).

SEM analysis results showed that the membranes present a porous structure that facilitates the passage of metal cations.

The contact angles measured using a surface tensiometer for solids and liquids show that the CTA+PMMA+DOP+(D2EHPA/TOPO) and PMMA+DOP+(D2EHPA/TOPO) membranes are hydrophilic, which facilitates the transfer of ions. In contrast, CTA+DOP+(D2EHPA/TOPO) is hydrophobic, which is essential for separating and removing metals from aqueous solutions. Their ability to repel water, while interacting with hydrophobic substances makes them particularly effective for these applications.

Fourier-transform infrared (FTIR) spectroscopy confirmed the existence of specific interactions between the different constituents of the membranes produced. These interactions were evidenced by disruptions in certain characteristic bands, such as the narrowing and widening of the bands, as well as the appearance of new bands.

The thermal behavior of the various membrane materials was studied using thermogravimetric analysis (TGA). The results indicated that all the

developed membranes exhibit good thermal stability, withstanding temperatures up to 178 °C. This temperature is significantly higher than those typically used in different membrane processes.

The results demonstrated that the tree membranes synthesized are highly effective in immobilizing lead and copper. The incorporation of ethylenediamine tetraacetic acid (EDTA) in the strip compartment of the metal ion transport setup reveals marked variations in the efficiency of the membranes.

The membrane CTA+PMMA+DOP+(D2EHPA/TOPO 1:1) demonstrates a moderate capacity to influence Pb(II) and Cu(II) concentrations, suggesting a complex interaction with EDTA, which can form stable complexes with these metal ions. In contrast, the membrane CTA+DOP+(D2EHPA/TOPO 1:1) maintains low concentrations of these ions, indicating high efficiency in the presence of EDTA, potentially due to a greater affinity for forming complexes with metals. For the PMMA+DOP+(D2EHPA/TOPO1:1) membrane, moderate efficiency is observed for Pb(II), with a slight increase in Cu(II), suggesting selective interactions with EDTA, depending on the nature of the constituent polymers. Thus, the effect of EDTA on membrane performance underscores the crucial importance of specific chemical interactions in developing effective methods for heavy metal separation and purification.

These results highlight the importance of specific chemical interactions between the membrane, the extractants, and the complexing agent to optimize the separation process. Thus, these membranes offer a promising solution for the recovery and treatment of heavy metal-contaminated waters, paving the way for sustainable and efficient industrial applications.

REFERENCES

- ¹ A. A. Wao, S. Khare and S. Ganguli, *J. Environ. Human.*, **1**, 2373 (2014)
- ² G. Tepanosyan, L. Sahakyan, O. Belyaeva, S. Asmaryan and A. Saghatelian, *Sci. Tot. Environ.*, **639**, 900 (2018), <https://doi.org/10.1016/j.scitotenv.2018.05.21>
- ³ M. Bost, S. Houdart, M. Obeli, E. Kalonji and J. F. Huneau, *Biochem. Biophys. Res.*, **460**, 549 (2015), <https://doi.org/10.1016/j.jtemb.2016.02.006>
- ⁴ G. K. Kinuthia and K. Ali, *Sci. Rep.*, **10**, 8434 (2020), <https://doi.org/10.1038/s41598-020-65359-5>
- ⁵ E. M. Vrijenhoek, S. Hong and M. Elimelech, *J. Membr. Sci.*, **188**, 115 (2001), [https://doi.org/10.1016/S0376-7388\(01\)00376-3](https://doi.org/10.1016/S0376-7388(01)00376-3)

- ⁶ D. Zioui, O. Arous, N. Mameri, H. Kerdjoudj, M. S. Sebastian *et al.*, *J. Hazard. Mater.*, **336**, 188 (2017), <https://doi.org/10.1016/j.jhazmat.2017.04.035>
- ⁷ H. Briki, N. Abdellaoui, O. Arous, F. Metref and D. E. Akretche, *Cellulose Chem. Technol.*, **56**, 1109 (2022), <https://doi.org/10.35812/CelluloseChemTechnol.2022.56.99>
- ⁸ T. Tran, Y.-C. Tu, S. Hall-Laureano and C. Lin, *Ind. Eng. Chem. Res.*, **59**, 5307 (2020), <https://doi.org/10.1021/acs.iecr.9b04661>
- ⁹ V. Eyupoglu and R. A. Kumbasar, *J. Separ. Sci. Technol.*, **49**, 2485 (2014), <https://doi.org/10.1080/01496395.2014.938167>
- ¹⁰ G. M. Ritcey and A. W. Ashbrook, "Solvent Extraction – Principles and Applications to Process Metallurgy", Elsevier, Amsterdam, 1984, Part 1, p. 362
- ¹¹ M. Ahmadipour, F. Rashchi, B. Ghafarizadeh and N. Mostoufi, *J. Separ. Sci. Technol.*, **46**, 2305 (2011), <https://doi.org/10.1016/j.seppur.2004.07.006>
- ¹² L. Charerntanyarak, *Water Sci. Technol.*, **39**, 135 (1999), <https://doi.org/10.2166/wst.1999.0642>
- ¹³ N. A. A. Qasem, R. H. Mohammed and D. U. Lawal, *J. Clean Water*, **4**, 36 (2021), <https://doi.org/10.1038/s41545-021-00127-0>
- ¹⁴ A. Dbrowski, Z. Hubicki, P. Podkocielny and E. Robens, *J. Chem.*, **56**, 91 (2004), <https://doi.org/10.1016/j.chemosphere.2004.03.006>
- ¹⁵ J. H. Park, Y. S. Ok, S. H. Kim, J. S. Cho, J. S. Heo *et al.*, *J. Chem.*, **142**, 77 (2016), <https://doi.org/10.1016/j.chemosphere.2015.05.093>
- ¹⁶ B. L. Martins, C. C. Cruz, A. S. Luna and C. A. Henriques, *Biochem. Eng. J.*, **27**, 310 (2006), <https://doi.org/10.1016/j.bej.2005.08.007>
- ¹⁷ E. Katsou, S. Malamis, K. J. Haralambous and M. Loizidou, *J. Membr. Sci.*, **360**, 234 (2010), <https://doi.org/10.1016/j.chemosphere.2010.10.022>
- ¹⁸ J.-M. Arana Juve, F. Munk, S. Christensen, Y. Wang and Z. Wei, *J. Chem. Eng.*, **435**, 134 (2022), <https://doi.org/10.1016/j.cej.2022.134857>
- ¹⁹ A. Ö. Saf, S. Alpaydin and A. Sirit, *J. Membr. Sci.*, **283**, 448 (2006), <https://doi.org/10.1016/j.memsci.2006.07.023>
- ²⁰ M. Rzelewska-Piekut and M. Regel-Rosocka, *Phys. Sci. Rev.*, **8**, 937 (2021), <https://doi.org/10.1515/psr-2021-0049>
- ²¹ N. M. Kocherginsky, Q. Yang and L. Seelam, *Separ. Purif. Technol.*, **53**, 171 (2007), <https://doi.org/10.1016/j.seppur.2006.06.022>
- ²² L. D. Nghiem, P. Mornane, I. D. Potter, J. M. Perera, R. W. Cattrall *et al.*, *J. Membr. Sci.*, **281**, 7 (2006), <https://doi.org/10.1016/j.memsci.2006.03.035>
- ²³ R. Tayeb, C. Fontas, M. Dhahbi, S. Tingry P. Seta *et al.*, *Separ. Purif. Technol.*, **42**, 189 (2005), <https://doi.org/10.1016/j.seppur.2004.07.006>
- ²⁴ M. I. G. S. Almeida, R. W. Cattrall and S. D. Kolev, *Anal. Chim. Acta*, **987**, 1 (2017), <https://doi.org/10.1016/j.aca.2017.07.032>
- ²⁵ B. Alcalde, E. Anticó and C. Fontàs, *Appl. Sci.*, **11**, 10404 (2021), <https://doi.org/10.3390/app112110404>
- ²⁶ S. D. Kolev, Y. Baba, R. W. Cattrall, T. Tasaki, N. Pereira *et al.*, *Talanta*, **78**, 795 (2009), <https://doi.org/10.1016/j.talanta.2008.12.047>
- ²⁷ D. Kazemi and M. Reza Yafian, *J. Sci. Rep.*, **14**, 11622 (2024), <https://doi.org/10.1038/s41598-024-62401-8>
- ²⁸ S. Bahrami, M. R. Yafian, P. Najvak, L. Dolatyari, H. Shayani-Jam *et al.*, *Separ. Purif. Technol.*, **250**, 117 (2020), <https://doi.org/10.3390/membranes12010090>
- ²⁹ S. Zhao, A. Samadi, Z. Wang and J. M. Pringle, *J. Chem. Eng.*, **481**, 148792 (2024), <https://doi.org/10.1016/j.cej.2024.14879>
- ³⁰ M. Sugiura, M. Kikkawa and S. Urita, *Separ. Sci. Technol.*, **22**, 2263 (1987)
- ³¹ M. Sugiura, *Separ. Sci. Technol.*, **28**, 1453 (1993), <https://doi.org/10.1080/01496399308018050>
- ³² S. Mesrouk and F. Sadi, *Cellulose Chem. Technol.*, **58**, 169 (2024), <https://doi.org/10.35812/cellulosechemtechnol.2024.58.17>